Research & Reviews: Journal of Material Sciences e-ISSN: 2321-6212

Graphitic Carbon Nitride Based Composites as Advanced Photocatalysts from Synthesis to Application: A Review

Charles K Bandoh[1,2], Eric S Agorku[2*], Francis K Ampong[3]

[1]Department of Chemical Sciences, University of Energy and Natural Resources, Sunyani, Ghana
[2]Department of Chemistry, Kwame Nkrumah University of Science and Technology, Kumasi, Ghana
[3]Department of Physics, Kwame Nkrumah University of Science and Technology, Kumasi, Ghana

Review Article

Received: 07-Apr-2022, Manuscript No. JOMS-22- 48327;
Editor assigned: 09- Apr -2022, PreQC No. JOMS -22-48327(PQ);
Reviewed: 21- Apr -2022, QC No. JOMS -22-48327;
Revised: 23- Apr -2022, Manuscript No. JOMS -22-48327(R);
Published: 30- Apr -2022, DOI: 10.4172/2321-6212.10.4.001.
***For Correspondence:**
Eric S Agorku, Department of Chemistry, Kwame Nkrumah University of Science and Technology, Kumasi, Ghana

E-mail: seaky2k@gmail.com
Keywords: Photocatalysis; Graphitic carbon nitride; Semiconductors; Bandgap; Sunlight

ABSTRACT

In the search for an effective semiconductor for photocatalytic applications, certain important necessities such as narrow bandgap for efficient absorption of visible light, suitable band location for an effective redox reaction, low recombination rate, etc. need to be kept in mind. It is apparently clear that a no single semiconductor can satisfy these requirements. Graphitic Carbon Nitride (g-C_3N_4)-based semiconductor nanocomposites have however been found to possess these all-important qualities. This study outlines the most recent developments in the design and fabrication of g-C_3N_4-based materials, as well as their applications in photo catalysis.

INTRODUCTION

The expanding worldwide emergency of energy deficiency and natural issues are getting to be genuine dangers to the economic improvement of human society. Governments and researchers are working behind the clock to find green technologies as justifiable ways to solve these abovementioned crises [1]. Solar energy is an ideal source of energy to solve these energy crises without imposing any negative effects on the environment. This is because solar energy is environmentally friendly, and has limitless supply of power. Solar energy/sunlight has also been found

useful in the removal of pollutants [2]. Nowadays, scientific and engineering interest in semiconductor application has grown extensively. Especially, semiconductor-based photocatalysis has been considered as a renewable, economic, secure, and clean innovation, which conducts catalytic responses for an assortment of applications, such as water purification [3-6] lessening of CO_2 [7-9], evacuation of natural poisons [10,11], bacteria dis-infection [12,13], NOx abatement [14,15], and particular blend of organic compounds [16]. However, the less effectiveness in utilizing solar-energy still stay the blockage of semiconductor photocatalysts to fulfill the prerequisites of real-world applications [17]. For example, the traditional semiconductors (such as TiO_2, ZrO_2, ZnO, ZnS, and Fe_2O_3) perform poorly under visible light due to their large energy gap. For this reason, several modification have been made to these traditional semiconductors, as well as fabricating their alternatives [18-20].

Presently, how to design novel photocatalysts that are firm, abundant and simplistic in construction still remains a challenge. Effective use of solar energy, designing and manufacturing of semiconductor materials for photocatalysis application is widely studied by scientific researchers [21]. It is against this background that graphitic Carbon Nitride (g-C_3N_4) based semiconducting materials having caused waves of eagerness in the arena of scientific research due to its treasure of striking properties [22]. Graphitic Carbon Nitride (g-C_3N_4) is the most stable allotrope of carbon nitrides at ambient atmospheric conditions with unique surface properties that makes it suitable for many applications, including catalysis. As the saying goes, "there are more room for improvement", it is believed that, new physical properties of g-C_3N_4 nanocomposites are yet to be discovered. Since a single semiconducting material cannot meet the current demand, there is urgent need to develop various synthetic procedures and physicochemical strategies to enrich g-$C_3N_4$with a desired electronic structure, crystal structure, nanostructure, and heterostructure [23]. In this review, synthesis and applications of graphitic carbon nitride-based semiconductor composites are dealt with.

LITERATURE REVIEW

Graphitic Carbon Nitride (g-C_3N_4)

In 1989, Liu and Cohen projected that carbon nitride could be fabricated to be ultrahard materials. Nitrites of carbon are group of polymeric material comprising basically of carbon and nitrogen [24]. They can be gotten from carbon materials, through substitution of the carbon iotas by nitrogen, and gotten to be engaging candidates for an assortment of applications. As mentioned earlier, Graphitic Carbon Nitride (g-C_3N_4), in recent times has generated a lot of interest among researchers in the field of photocatalysis. This is due to the fact that g-C_3N_4 is chemically stable and has exceptional microelectronic band structure [25], the occurrence of basic sites, low cost, metal free, and very responsive to visible light. It is estimated through thermogravimetric investigation that carbon nitrides can endure heat up to 600°C and will decompose wholly when temperatures rises to 750°C [26].

Ideally, g-C_3N_4comprises exclusively an assemble of C-N bonds in which there are no localisation of electrons in π state [27]. The ability of graphitic carbon nitride to undertake structural and chemical alteration gives it a plausibility of fine tuning its structure and reactivity and allows one to control the semiconducting properties and altogether expand the variety of catalytic applications [28]. Additionally, g-C_3N_4 is a polymeric semiconductor with an exceptional structure, energy gap of 2.7 eV and amazing physical and chemical properties [29]. G-C_3N_4 possesses strong van der Waals forces among its layers which make it chemically stable in most solvent such as alcohols, water, diethyl

ether, toluene, N, N-dimethylformamide, and tetrahydrofuran. More critically, g-C_3N_4 is as it were composed of two earth-abundant components: carbon and nitrogen. This proposes that it can effectively be produce at a low cost, and that its properties can be tuned by straightforward techniques without critical modification of what it's generally made of [30].

In spite of the above mentioned benefits of g-C_3N_4, there is high rate of recombination of charge carriers generated by photo reactivity which limit the photocatalytic efficiency [9] and low electrical conductivity. In an attempt to curb the just mentioned problems associated with g-C_3N_4, researchers capitalised on its compatibility with several inorganic nanoparticles [1] to fabricate g-C_3N_4-based composite materials. Several approaches such as metal doping [31,32], non-metal doping [33-35], metal/non-metal co-doping [36], fabrication of nano/mesoporous structure [37] and combining with other semiconductors [38], have been use to enhance the photocatalytic performance of g-C_3N_4 [39].

Graphitic Carbon Nitride (g-C_3N_4)-based semiconductor nanocomposites

In the search for effective g-C_3N_4-based nanocomposites, certain important necessities such as narrow band gap for efficient absorption of visible light, suitable band location for an effective redox reaction, etc. need to be kept in mind. It is apparently clear that a no single semiconductor can satisfy these requirements [40]. It is on the bases of this that several semiconducting materials such as CdS [41], WO_3 [42], $BiWO_6$ [43], ZnO [44], TiO_2 [45], Ag_2O [46], Cu_2O [47], Fe_2O_3 [48], In_2O_3 [49], graphene [50] and carbon quantum dots were coupled with g-C_3N_4 to fabricate composites [26]. Construction of g-C_3N_4 based heterostructured composites endow the composites with the ability to conquer the recombination of photoinduced charge carriers, and also enhanced the composite with physicochemical properties [46].

Synthesis Graphitic Carbon Nitride (g-C_3N_4)

In 2009, Wang and co-workers discovered that graphitic carbon nitride can be used to produce H_2 from water [51]. Since then, several efforts have been made to manufacture g-C_3N_4 semiconductor and its derivatives by thermal condensation of plentiful, nitrogen-rich and oxygen-free precursors which contain C–N bonds [52,53]. Nitrogen-rich precursors (Figure 1) such as urea [54], thiourea [55], melamine [7,56], cyanamide [57-59], dicyandiamide [59,60]have been used to synthesise g-C_3N_4.

Figure 1. Shematic diagram of the synthesis of graphitic carbon nitride by thermal condensation [61].

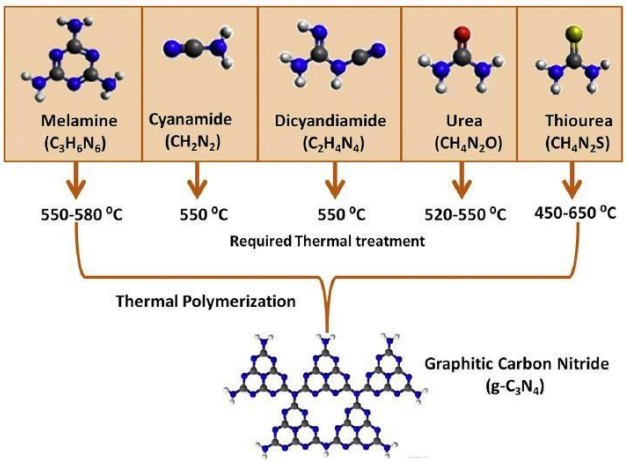

Several authors have reported that physical and chemical properties of g-C_3N_4 such as surface area, porosity, absorption, photoluminescence, C–N ratio, and nanostructures are strongly influenced by the type of precursors and treatment used [16]. This means that the choice of precursors and treatment methods are very crucial. For example, Zhang and co-workers prepared g-C_3N_4 by directly heating thiourea at varied temperatures for 2 h. They concluded that condensation temperature greatly affect formation of g-C_3N_4. However, increasing the temperature to 650°C accelerates the partial decomposition of the catalyst itself [62]. Cui et al. [63] also fabricated g-C_3N_4 by heating directly ammonium thiocyanate and dicyandiamide at different temperatures. XRD analysis of their samples revealed that the characteristic graphite-like structure of g-C_3N_4 evolves when the calcination temperature exceeds 450°C. They concluded that a sample obtained from ammonium thiocyanate was of improved photoactivity than those fabricated from dicyandiamide [63]. Additionally, Yan and co-workers successfully fabricated g-C_3N_4 by direct heating of melamine in a semi closed system with the aim of preventing sublimation of melamine. In their synthesis process, melamine powder was put into alumina crucible with a cover, then heated to 500 °C in a furnace for 2 h, and later subjected to deammonation treatment at 500, 520, 550, and 580°C for 2 h. It was evident from their analysis that, g-C_3N_4 is stable in the partly closed ammonia atmosphere than in the open system [64]. Studies conducted by Mo et al. on the effect of calcination temperature on crystal structure, morphology evolution, energy gap engineering of melamine-derived graphitic carbon nitride revealed that, g-C_3N_4 could be formed fully only when the calcination temperature exceeds 500°C. They also reported that samples fabricated at 650°C showed an extraordinary photocatalytic performance.

Synthesis of Graphitic Carbon Nitride (g-C_3N_4)-based semiconductor nanocomposites

In the quest to manufacture g-C_3N_4 based heterostructure, there are few things one ought to consider. First and foremost, the chosen semiconductors must have a reasonable band arrangement. Furthermore, the semiconductors got to be associated in such a way that their interesting physical and chemical properties are ideally utilized. The choice of a suitable blend methodology comes into play when the implementation and optimization of the heterostructure is the prime concern [65]. Several researchers have developed different ways to effectively synthesize g-C_3N_4-baesd nanocomposites. These include: simple calcination method, solution mixing, sol-gel, hydrothermal, hydrolysis, and microwave irradiation. According to Liu et al. these methods have been grouped into two major kinds of artificial approaches which have been employed for the synthesis of g-C_3N_4-based composites. Firstly, the material is mixed with carbon nitride precursor accompanied with thermal condensation at favourite temperature. Secondly, the material is post treated with as- prepared g-C_3N_4 by deposition or basically mixing). For example, Ghane et al. prepared Fe_2O_3/ g-C_3N_4 nanocomposites using the latter method. In their synthesis process, different amounts of Fe $(NO_3)_3.9H_2O$ and urea were added to as-prepared g-C_3N_4 powder. Optical absorption spectroscopy analysis of their samples showed an increase absorption in the visible region of the EM spectrum with increasing Fe_2O_3 content, which was proven by a decrease in bandgap from 2.65–1.75 eV. They concluded that, coupling g-C_3N_4 with Fe_2O_3 endowed the resulting composite with certain remarkable qualities such as electron-hole recombination reduction, efficient visible light harvesting, and energy gap narrowing. However, there was a word of caution from their report that, although increasing Fe_2O_3 content of the nanocomposite enhanced its photoresponse, excessive Fe_2O_3 content can undo the achievement made. Ge et al. on the other hand fabricated g-C_3N_4/Bi_2WO_6 composite by mixing the powders of as-prepared g-C_3N_4 and Bi_2WO_6. The resultant samples were collected and calcined at 300°C for an hour in a muffle furnace. Analysis of their samples revealed an efficient photocatalytic activity on MO degradation with degradation efficiency of 99.9%. This was attributed to

the synergic effect between polymeric g-C_3N_4 and Bi_2WO_6, which played a vital role in supressing electron-hole recombination.

Also, Chang et al. prepared g-C_3N_4–TiO_2 nanocomposite through simplistic sol–gel technique using tetra-n-butyl titanate as a precursor. This precursor undergoes hydrolysis and polycondensation process to form a colloid solution. Analysis of their samples revealed a close contact between g-C_3N_4 and TiO_2 to form a heterojunction structure.

Sol-gel method is one of the critical approaches that have been used to fabricate extremely permeable g-C_3N_4. Due to its low cost, ambient processing temperature, and synthesis route, sol-gel technique has been considered as one of the unique methods. This method has been known as one of the appropriate methods for the fabrication of g-C_3N_4 and metal oxides semiconductor photocatalysts due to the production of metal-OH network [66]. Recently, in the field of material science ceramic engineering, sol-gel method which is a wet-chemical process has been employed [67].

Doping

Metal doping: Junction formed between a semiconductor and a metal has been extensively used to generate space-charge separation region popularly known as Schottky barrier. In order to prevent charge recombination and also align Fermi energy levels, electrons transfer occurs from one component to the other at their interface. It is therefore possible to dope g-C_3N_4 with metals with the aim of increasing the photocatalytic activity. G-C_3N_4 has an exceptional structure, with nitrogen forming a triangle (Figure 2). Each of the triangles has six lone-pair electrons which makes it very easy for metal incorporation into the structure [25]. Doping g-C_3N_4 with a metal endows it with low energy gap, improved surface area, high absorption of visible light and prevention/reduction of recombination of light generated electron-hole pairs [68]. To be able to incorporate metal ions into the network of g-C_3N_4, the g-C_3N_4 precursor is mixed uniformly with the soluble salt that contains the metal ions. Through thermal condensation of precursor, metal impurities will be concurrently doped into the network of the g-C_3N_4 [69].

Figure 2. Structure of graphitic carbon nitride [70].

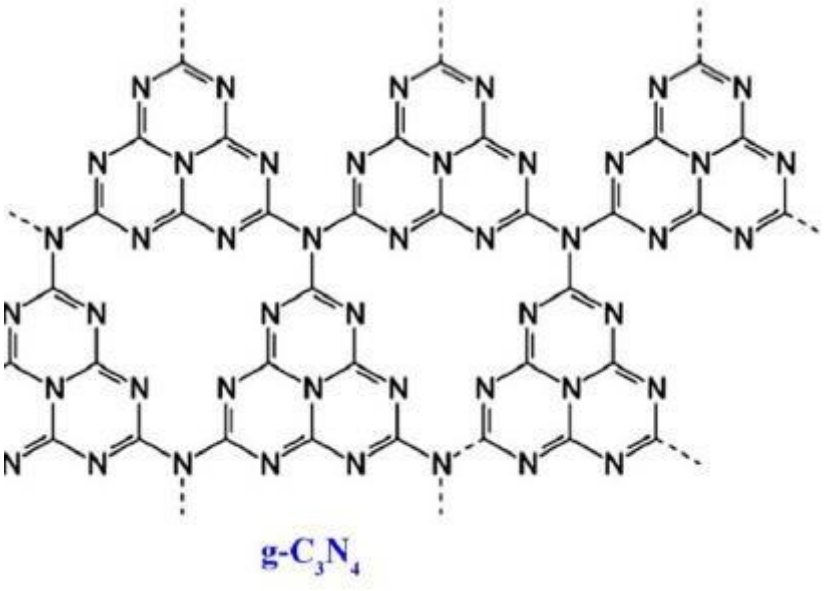

Several metals such as Fe, Zn, Cu, Co, Ag, Li, K, Ni, Na, Er, V, etc. have been used to dope g-C_3N_4 photocatalyst with the aim of modulating its physical and chemical properties [71-78]. In general, one of the effective strategies to enhance the performance of g-C_3N_4 through modification of its electronic structure and surface properties is by

elemental doping [79]. For example, Das and co-workers fabricated Nickle doped g-C_3N_4 using urea and nickel nitrate hexahydrate as precursors [80]. As revealed in Figure 3, the Ni ions may be synchronised with the large rings of C–N. Moreover, they reported that, when Ni atoms are introduced into the structure, many states are created within the energy gap and also there was an electronic bond between the Ni atoms and the lone pairs of nearby nitrogen atoms. They also reported a reduction in the recombination rate of photogenerated carriers. They attributed this to the fact that electrons spend some time being trapped in the doping site, thereby prolonging the time taking by an electron to recombine with a hole. It was evident from their research that band gap decreased with increasing doping concentration.

Figure 3. Possible doping site for Ni. (Note: - Nitrogen, -Carbon, -Ni^{2+})

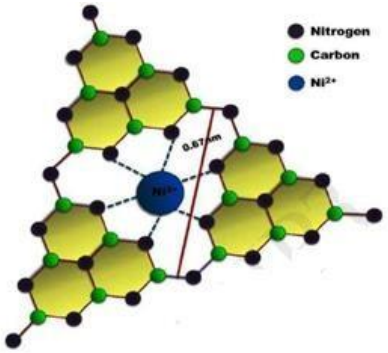

Reddy et al. performed photochemical studies on Ni–doped g-C_3N_4 nanostructures under visible light and presented similar report as Das et al.

Fronczak et al. [81] fabricated undoped and Na-doped g-C_3N_4 by thermal condensation using sodium chloride and cyanamide as precursors. They reported that the Na-doped g-C_3N_4 samples had an exceptional adsorption performance (with maximum adsorption ability in the range between 200 and 300 $mg.g^{-1}$) in relation to the removal of an anionic dye-methyl blue.

Additionally, Zhao's group presented a novel energy gap-tunable K-Na co-doped g-C_3N_4 photocatalysts by molten salt method using melamine, potassium chloride and sodium chloride as precursors. They reported that when the weight ratio of eutectic salts to melamine is controlled, the conduction band and the valence band potentials of g-C_3N_4 can be tuned from -1.09 and +1.55 eV to -0.29 and +2.25 eV respectively [82]. This will surely lead to the formation of *OH and $*O_2$ resulting into a much higher photodegradation rate. Zhao et al. added that K-Na co-doping endows the g-C_3N_4 photocatalyst with a supressed crystal growth, enhanced surface area and a decreased electron-hole recombination. Similar results were obtained by Hu and friends when they synthesized Fe-P co-doped g-C_3N_4 photocatalyst with dicyandiamide monomer, ferric nitrate, and diammonium hydrogen phosphate as reacting chemicals [32]. The extraordinary performance of their samples was attributed to synergistic effect of Fe and P co-doping.

In summary, there has been a widespread introduction of metal ion dopants into the structure of g-C_3N_4. Some of the benefit of metal ion dopants is the creation of new energy levels in the energy gap, improved visible light response, and an increased electron-hole separation rate.

Non-metal ion doping: G-C_3N_4 is known to be a very promising metal-free polymeric photocatalyst [4]. In an attempt to maintain the metal-free characteristics of g-C_3N_4, much attention of researchers has been drawn to no-metal doping. Unlike metals, non-metals have high ionization energies and high electronegativity which offer them the

ability to form covalent bonds. More importantly, non-metals can overcome thermal variation of chemical states of doped metal ions. It is believed that introducing non-metal ions into graphitic carbon nitride could endow the system with a unique electronic structure and bandgap that can be tuned for a desired application such as Photoluminescence (PL) [34].

Different non-metals such as P [83], B [77], S [84] and Br [54] have been extensively used to dope g-C_3N_4. For example, boron doped g-C_3N_4 photocatalysts were fabricated by Lu and friends using thiourea and boric acid as precursors. They reported that introducing B atoms into g-C_3N_4 structures enhances its photocatalytic activities by lowering its band gap with a corresponding high absorption of visible light. They performed photocatalytic degradation activities on UO22+ and reported 93% efficiency. After evaluating the long-term stability of their samples, it was observed that the samples were very stable even after five cycles [77]. In addition to altering the bandgap, boron doping can modify the conductivity of g-C_3N_4 from n-type to p-type whereas keeping the conduction band edge negative sufficient for hydrogen generation [85].

In 2015, Zhou et al. presented an excellent work on P-doped g-C_3N_4 by a thermo-induced copolymerization approach with Guanidiniumhydrochloride (GndCl) and hexachlorocyclotriphosphate as P source. In their preparation process, 5 g of guanidiniumhydrocloride was made into powdered form and mixed with different quantities of hexachlorocyclotriphosphate. This combination was then put into a furnace and heated to a desired temperature (550, 600, 650°C) at the rate of 2°C per minutes. They investigated the photocatalytic performance, and rhodamine B decomposition of the resulting P-doped g-C_3N_4 photocatalyst completely degraded 10 mgL^{-1} RhB in 10 min, whereas pure g-C_3N_4 will need 30 min. They moreover, reported H_2 evolution rate of 50.6 µmol h^{-1}, which is 2.9 times greater than that of pure g-C_3N_4.

Additionally, Zhou and friends stated that adding P atoms to g-C_3N_4 positively affect electronic, semiconducting, and chemical properties of g-C_3N_4. Again, they detailed that there was efficient suppression of recombination of light generated electrons and holes.

In similar study, Wang et al. [86] also fabricated P-doped g-C_3N_4 nanosheets for the detection of silver ion and cell imaging. Melamine and diammonium hydrogen phosphate were the precursors used. In their approach, a suspension was formed by adding the precursors to water in a beaker. After heating in an oil bath at 100°C for 2 hours and removing the water, the solids were dried in an oven at 100°C for 2 hours. The product was calcined for 4 hours at 520°C at 2°C/min in an alumina crucible. To obtain bulk P-doped g-C_3N_4, the yellow solid was ground into powder, which was then dissolved in water and ultrasonically dispersed for 12 hours. Centrifugation and lyophilization were used to collect solid P-doped g-C_3N_4 nanosheets. In addition to B-doped and P-doped graphitic carbon nitride photocatalysts, Br-modified g-C_3N_4 semiconductors have also been prepared by Lan, et al. [54] for photoredox water splitting. Urea (10 g), and with different concentration of ammonium bromide (NH_4Br) was mixed with 10 mL deionized water while stirring to remove water. The products were sintered at 550°C for 2 h at a heating rate of 5.0°C/min in air. Other chemicals such as dicyandiamide, ammonium thiocyanide and thiourea were used in conjunction with ammonium bromide to fabricate Br-doped g-C_3N_4 *via* similar method. They reported that, the addition of bromine to g-C_3N_4 modifies the texture, optical absorption, electrical conductivity, charge-carrier transfer rate, and photocatalytic efficiency without damaging the polymer's major structure and architecture.

Sulphur, being one of the nonmetallic elements has also been used to dope graphitic carbon nitride. Zhang et al. fabricated S-doped g-C_3N_4 *via* a simple method. Three (3) g of melamine was mixed with varied amount of elemental sulphur. The mixture was grounded into powder and then transported into a covered crucible and heated to 650°C for 2 hours directly in nitrogen gas. Optical absorption spectroscopy analysis of their sample revealed a bandgap decrease from 2.76–2.58 eV for a pure g-C_3N_4 and sulphur-doped g-C_3N_4 respectively. The observed red shift and additional absorption into longer wavelength for all S-doped g-C_3N_4 was attributed to intermediate energy bands related to surface imperfections induced by sulphur mediated fabrications. It was evident from their PL analysis that charge carrier recombination was efficiently supressed by the S-doped g-C_3N_4 due to optimized structure, electronic and a textural property that assists charge separation.

Jiang and friends studied the combined effect of co-doping g-C_3N_4 with sulphur and phosphorus on photocatalytic performance for the degradation of methyl orange and tetracycline. Co-doping has been found to combine the advantages of both impurity atoms, resulting in the enhancement of the photocatalytic performance. In their synthesis approach, varied amount of Hexachlorotriphosphazene (HCCP) and fixed amount of thiourea were mixed together, grounded into powder and calcined for 4 hours at 550°C in a covered crucible where the heating rate was kept at 10°C/min. After cooling to room temperature, the resulting products were gathered and grounded into powder. They reported that the P-, S-codoped g-C_3N_4 had significantly higher visible light photocatalytic activities against TC and MO solution than pure g-C_3N_4 and single-doped g-C_3N_4. They added that P-S-co-doped g-C_3N_4 enhances surface area, light absorption ability, and charge separation efficiency, thereby leading to higher photoactivity.

Zhang et al. [87] has also described the synthesis of B and P co-doped g-C_3N_4 nanosheets for organic waste removal. BmimPF6, B_2O_3 and melamine were the precursors used. In their methodology, 50 mg BmimPF6, 50 mg B_2O_3 and 3 g melamine were introduced into 15 mL water. Whiles constantly being stirred, the resulting suspension was heated at 100°C for the removal of water. To obtain the dark yellow bulk B, P co-doped g-C_3N_4; the product was grounded, transferred into a covered crucible and heated at 520°C for 4 hours in an oven. For the B, P co-doped g-C_3N_4 nanosheets, the authors adopted a simple method called direct thermal oxidation etching process, which was developed by Niu, et al. [88]. The bulk B, P co-doped g-C_3N_4 was placed in a crucible without a cover and heated at 500 °C at a rate of 5°C/ min for 2 hours to obtain a light-yellow sample. The results of their analysis were similar to that of Jiang et al. described above.

In a nut shell, doping plays a vital part in tuning the electronic band structure of g-C_3N_4. Metal doping happens through inclusion into the system of g-C_3N_4, whereas non-metal doping happens by means of substitution of carbon or nitrogen atoms, which influences the resulting conduction band and valence band. Almost all the time, a diminished bandgap can be achieved, leading to an increase in the light absorption capacity. This is often very adaptable technique that empowers the bandgap designing of g-C_3N_4 by choosing particular doping elements and their quantities, depending upon the specified band positions [1].

Application

A wide range of g-C_3N_4-based photocatalysts have been used in redox reactions as diverse as water splitting, CO_2 reduction, pollutants degradation, bacterial inactivation, solar energy conversion, organic synthesis, and photoelectronic system fabrication [52,85,89-91].

Water splitting: The basis of natural photosynthesis is focused on the analysis of H_2 and O_2 generation from water splitting by semiconductor-based photocatalysts. The production of O_2 is difficult [92]. Photolysis of water needs semiconductors with conduction bands with more negative potential for reducing H+ to H_2, while their valence bands must exhibit a more positive potential than the potential necessary for oxidizing H_2O to O_2 [93]. Most g-C_3N_4 photocatalysts are only used in the semi reactions of H_2 or O_2 evolution because the formation of O_2 necessitates a four-electron transfer phase that demands a significant overpotential [92].

Qin et al. [90] fabricated Zn-doped g-C_3N_4/$BiVO_4$ z-scheme photocatalyst combination to split water completely into H_2 and O_2. The system comprises Fe^{3+}/Fe^{2+} redox mediator for water splitting whereby Zn-doped g-C_3N_4 was used for H_2 evolution and $BiVO_4$ for O_2 evolution. Moreover, the photocatalyst for H_2 generation ought to have great charge division execution and an adequate oxidation energy level to oxidize halfway particles to an elevated valence state, so as to guarantee the smooth realization of another half reaction. It ought to be noted that there are numerous components influencing the redox cycle of the intermediary medium, just like the adjustment of pH and the inclusion of appeasing agent, which may cause harm to the charge exchange structure so as to obstruct the catalytic performance [92]. Additionally, Thaweesak and friends manufactured B-doped g-C_3N_4 nanosheets for improved visible light photocatalytic water splitting. The structure of nanosheets can provide surface catalytic active area and also reduces the distance with which the photoexcited charge carriers defuses from the bulk to the surface [89]. In 2016, Lan and co- workers prepared bromine-modified graphitic carbon nitride photocatalysts for water splitting through one-pot condensation of urea and NH_4Br. Photocatalytic water reduction analysis of the Br-modified g-C_3N_4 samples revealed a comparatively high evolution rate for H_2, i.e., 48 $\mu molh^{-1}$ as against 20 $\mu molh^{-1}$ for pure g-C_3N_4. However, this was not the same for water oxidation process for O_2 production. Br-modified g-C_3N_4 samples showed restricted activity for O_2 evolution (4 $\mu molh^{-1}$). This was attributed to the fact that the VB edge of the Br-g-C_3N_4 was not positive sufficient to drive the numerous electron/energy exchange process of O_2 production. Furthermore, the huge O_2 evolution over-potential and poor surface kinetics constantly slowed down the water oxidation cycle. To overcome these challenges, cobalt oxide was loaded on g-C_3N_4 as co-catalyst for water oxidation. This resulted to O_2 production rate of about 6 times more than that of pure Br-g-C_3N_4 [54].

Generally, the key to the complete water splitting by photocatalysis is that its redox procedures ought to have comparatively high photocatalytic carrier separation rate, whether a single catalyst or a separation system composed of two catalysts [92].

CO_2 photoreduction: Carbon dioxide gas photoreduction has been a major topic of research in the fields of environment and energy as the global greenhouse effect has intensified [94]. CO_2 is chemically reduced into hydrocarbons using photocatalytic technology, which not only converts this greenhouse gas into recycled fuel but also helps to reduce global warming. CO_2, on the other hand, is a very stable compound, making direct reactions difficult. The solar photocatalytic transformation of CO_2 to hydrocarbon fuels in the presence of H_2O has gotten a lot of attention because it has the potential to reduce society's current reliance on fossil fuels while also lowering CO_2 levels in the atmosphere and thus lowering the greenhouse effect [95]. Several methods such as doping, heterostructures, cocatalyst loading and fabrication of z-scheme have been employed to improve the photocatalytic activity of g-C_3N_4 for CO_2 reduction [85,96-99]. For instance, Cao and friends reported a facet effect of Pd co-catalyst on photocatalytic CO_2 reduction over g-C_3N_4. It was evident from reduction process that the tetrahedral palladium nanocrystals with exposed (111) facets were more effective co-catalyst than the cubic. This structural dependent

CO_2 photoreduction activity was primarily ascribed to the more preferable electron sink effect, CO_2 adsorption ability and CH_3OH desorption ability of the Pd(111) surface. They further explained that deposition of Pd nanocrystals on g-C_3N_4 can capture photogenerated electrons from the CB of g-C_3N_4 *via* such Pd/g-C_3N_4 heterojunction. The collected electrons on the Pd nanoparticles in this way respond to the surface-adsorbed CO_2 and H+ to create CH_3OH and CH_4 gas, whereas H_2O particles devour holes to discharge O_2 and H+ within the valence band of g-C_3N_4 [96].

More recently, Guo et al. constructed a z-scheme g-C_3N_4/Bi_2O_2 [BO_2 (OH)] photocatalyst through a facile high-energy ball grinding approach, with close interfacial interaction between g-C_3N_4 and Bi_2O_2 [BO_2 (OH)]. The obtained heterogenous semiconductor photocatalyst showed a remarkable performance for CO_2 photoreduction. They reported that the improved photocatalytic activity was mainly accredited to the largely assisted charge carrier separation and supressed recombination. This was made possible due to the formation of the z- scheme band structure. In 2018, a novel ternary Ag_2CrO_4/g-C_3N_4/GO nanocomposite z-scheme photocatalyst was synthesized by Xu and friends for CO_2 photoreduction into CH_3OH and CH_4. Ag_2CrO_4 and GO were employed as photosensitizer and co-catalyst respectively. They stated that the ternary photocatalyst attained a CO_2 reduction activity of 1.03 $\mu molg^{-1}$ and a turn over frequency of 0.30 h^{-1}, which according to them was 2.3 times higher that of pristine g-C_3N_4. The improved photocatalytic activity was credited to extended light absorption, advanced adsorption of CO_2 and more effective charge separation, which resulted from the well-matched band structure of the z-scheme and an appropriate loading ratio of silver chromate. Mostly, a well-matched band structure is a criterion for the development of a z-scheme structure [97]. Xu and friends further stated that, when GO is used as a cocatalyst, it champions the charge carrier transfer and also offers more CO_2 adsorption and catalytic sites [100]. Silver bromide/graphitic carbon nitride (AgBr/g-C_3N_4) nanocomposite photocatalyst has also been prepared by Murugesan et al. [101] *via* modified deposition-precipitation technique for CO_2 photoreduction into methane and acetone. Silver nitrate, melamine and trimethyl-ammonium bromide were the precursors used. Their report revealed that the AgBr/g- C_3N_4 composite showed an improved photocatalytic activity for photoreduction of CO_2 in aqueous medium under UV light than the pure g-C_3N_4. Parameters such as pH, reaction medium, irradiation time and catalyst dosage were studied, and were found to influence the reduction of CO_2.

Dyes and organic pollutants decomposition: Clean and non-polluted water is one of the basic requirements for all living organisms including human beings. It is also a critical feedstock to a variety of key industries including food and pharmaceuticals. But its availability is a major issue nowadays. In the future, this issue will further increase due to global industrialization and population growth [6]. Currently, photodegradation of organic pollutants *via* g-C_3N_4 based semiconductors has attracted the attention of researchers [102].

Chai et al. [103] fabricated P-doped g-C_3N_4 *via* co-polycondensation technique for photodecomposition of Rhodamine B (RhB). The P-g-C_3N_4 exhibited an enhanced photocatalytic activity towards RhB than the pure g-C_3N_4 under visible light irradiation. They recorded maximum removal efficiency of 95 % as against 67 % for pure g-C_3N_4 after 30 min. This was accredited to the substitution of P atoms for C atoms of g-C_3N_4 network resulting in the formation of π-conjugated scheme and improvement in light harvesting. Also, SnO_2-ZnO quantum dots have been anchored on graphitic carbon nitride nanosheets to form a ternary semiconductor for photoreduction of RhB. The obtained hybrid achieved photocatalytic efficiency of 99% in 60 min under visible light irradiation. The extraordinary

photoactivity was attributed to swift electron production and transfer driven by visible light due to robust interaction between SnO_2-ZnO quantum dots with g-C_3N_4 matrix [104].

Ge et al. [31] synthesized g-C_3N_4/Bi_2WO_6 heterostructure for the decomposition of methyl orange (MO) under visible light illumination. The optimized photocatalyst showed decomposition efficiency of 99.9% after 3 h of illumination. It was concluded that the enhanced photoactivity was due to the synergic effect between g-C_3N_4 and Bi_2WO_6, which played a significant role in supressing electron-hole pairs. Additionally, Konstas et al. [105] manufactured g-C_3N_4/$SrTiO_3$ heterostructure through sonication mixing for degradation of Methyl Blue (MB) under visible light illumination. The system showed an improved photoactivity towards MB degradation with about 95% efficiency. They credited this enhanced degradation performance to the formation of z-scheme mechanism. The photodecomposition of Malachite Green (MG) by Ag/ g-C_3N_4 photocatalyst showed that within 30 min 80% of the MG was removed as against 48 % for the pure g-C_3N_4 [106].

Type-II CeO_2/g-C_3C_4 nanosheets were produced by Ma et al. [107]and used to photocatalyzed the breakdown of Bisphenol A (BPA) under visible light irradiation. About 94% of BPA was removed by the CeO_2/g-C_3C_4 in 80 minutes, which was much greater than CeO_2 (14%) and g-C_3C_4 (65%). They reported that the CeO_2/g-C_3C_4 heterostructure possessed a well-matched energy bands which assisted the photogenerated charge carriers' migration and separation, thereby resulting in an enhanced photodegradation of BPA. Finally, because of the excellent photocatalytic characteristics of g-C_3N_4-based photocatalysts, photocatalytic destruction of organic matter provides an efficient technique to eradicate organic contaminants [108,109].

DISCUSSION AND CONCLUSION

Fundamentally, the goal of this review was to gather the prevailing approaches and alterations that have been employed to overcome the limitations of pure g-C_3N_4 for photocatalytic applications. Some of these limitations are, charge carrier recombination, low specific surface area, low absorption of visible light, poor quantum harvest and low recovery of photocatalyst. Synthesis approaches and possible photocatalytic applications have been discussed. The g- C_3N_4-based composites that were driven by visible light showed great promise in wastewater purification. The heterostructures of g-C_3N_4-based semiconductor photocatalysts have the potential to improve visible light absorption, chemical stability, charge migration and separation, and hence an enhanced photocatalytic performance.

In general, it is certain that there will be various interesting prospects on g-C_3N_4-based nanocomposites. It is anticipated that this review will give a few directions and deliver a few conclusions to those who are curious about g-C_3N_4-based nanocomposites.

REFERENCES

1. Cao S, et al. Polymeric photocatalysts based on graphitic carbon nitride. Adv Mater. 2015;27:2150-2176.
2. Jiang L, et al. Doping of graphitic carbon nitride for photocatalysis: A reveiw. Appl Catal B. 2017;217:388-406.
3. Liu B, et al. Phosphorus-doped graphitic carbon nitride nanotubes with amino-rich surface for efficient co2 capture, enhanced photocatalytic activity, and product selectivity. ACS Appl Mater Interfaces. 2004;10:4001-4009.

4. Cui Y, et al. Metal-free photocatalytic degradation of 4- chlorophenol in water by mesoporous carbon nitride semiconductors. Catal Sci Technol. 2012;2:1396-1402.
5. Jegatheesan V, et al. Bioresource technology treatment of textile wastewater with membrane bioreactor : A critical review. Bioresour Technol. 2016;204:202-212.
6. Kumar S, et al. Photocatalytic degradation of organic pollutants in water using graphene oxide composite. In A new generation material graphene: applications in water technology. Cham: Springer. 2018.
7. Ohno T, et al. Photocatalytic reduction of CO_2 over a hybrid photocatalyst composed of WO_3 and graphitic carbon nitride (g-C_3N_4) under visible light. J CO_2 Util. 2014;6:17-25.
8. Lin J, et al. Photochemical reduction of CO_2 by graphitic carbon nitride polymers. ACS Sustain Chem Eng. 2014;2:353-358.
9. Ong W, et al. Heterostructured AgX / g-C_3N_4 (X=Cl and Br) nanocomposites *via* a sonication-assisted deposition-precipitation approach : Emerging role of halide ions in the synergistic photocatalytic reduction of carbon dioxide. Appl Catal B. 2016;180:530-543.
10. Liu Y, et al. Novel visible light-induced g-C_3N_4-Sb_2S_3/$Sb_4O_5Cl_2$ composite photocatalysts for efficient degradation of methyl orange. Catal Commun. 2015;70:17-20.
11. Li Y, et al. Enhancing the sludge dewaterability by electrolysis/electrocoagulation combined with zero-valent iron activated persulfate process. Chem Eng. 2016;303:636-645.
12. Mitoraj D, et al. Visible light inactivation of bacteria and fungi by modified titanium dioxide. Photochem Photobiol Sci. 2007;6:642-648.
13. Xia D, et al. Visible-light-driven inactivation of Escherichia coli K-12 over thermal treated natural pyrrhotite. Appl Catal B. 2015;176–177:749–756.
14. Papailias I, et al. Enhanced NO_2 abatement by alkaline-earth modified g-C_3N_4 nanocomposites for efficient air purification. Appl Surf Sci. 2018;430:225-233.
15. Yang Y, et al. Photocatalytic NOx abatement and self-cleaning performance of cementitious composites with g-C_3N_4 nanosheets under visible light. Constr Build Mater. 2019;225:120-131.
16. Wang A, et al. Recent advances of graphitic carbon nitride-based structures and applications in catalyst, sensing, imaging, and LEDs. Micro Nano Lett. 2017;9.
17. Zhao Z, et al. Graphitic carbon nitride based nanocomposites: A review. Nanoscale. 2014 ;7:15-37.
18. Lui G, et al. Graphene-wrapped hierarchical TiO_2 nanoflower composites with enhanced photocatalytic performance. J Mater Chem A. 2013;1:12255-12262.
19. Dinkar AV, et al. Sm- Doped Tio_2 Nanoparticles with high photocatalytic activity for ars dye under visible light synthesized by ultrasonic assisted Sol-Gel method. Orient J Chem. 2016;32:933-940.
20. Xu Y, et al. Novel visible-light-driven Fe_2O_3/Ag_3VO_4 composite with enhanced photocatalytic activity toward organic pollutants degradation. RSC Advances. 2016;6: 3600-3607.
21. Durgalakshmi D, et al. Green photocatalyst for diverge applications. Springer Nature Switzerland AG. 2019.
22. Zhu J, et al. Graphitic carbon nitride: Synthesis, properties, and applications in catalysis. ACS Appl Mater Interfaces. 2014;6:16449-16465.
23. Zheng Y, et al. Graphitic carbon nitride polymers toward sustainable photoredox catalysis. Angewandte Chemie - International Edition. 2015; 54:12868-12884.
24. Liu AY, et al. Prediction of new low compressibility solids. Science. 1989;245:841-842.

25. Wang L, et al. Metal / graphitic carbon nitride composites : synthesis , structures , and applications. Chem Asian J. 2016;11:3305-3328.
26. Liu J, et al. Graphitic carbon nitride “reloaded”: Emerging applications beyond (photo)catalysis. Chem Soc Rev. 2016;45:2308-2326.
27. Su F, et al. mpg-C_3N_4 as a solid base catalyst for Knoevenagel condensations and transesterification reactions. Catal Sci Technol. 2012;2:1005-1009.
28. Akhmedov VM, et al. Synthesis, properties , and application of polymeric carbon nitrides. Russ Chem Bull. 2017;66:782-807.
29. Groenewolt M, et al. Synthesis of g-C_3N_4 nanoparticles in mesoporous silica host matrices. Adv Mater. 17:1789-1792.
30. Wang X, et al. Polymeric graphitic carbon nitride for heterogeneous photocatalysis. ACS Catal. 2012;2:1596-1606.
31. Ge L, et al. Novel visible light-induced g-C_3N_4/Bi_2WO_6 composite photocatalysts for efficient degradation of methyl orange. Appl Catal B. 2011;108–109:100-107.
32. Hu S, et al. Enhanced visible light photocatalytic performance of g-C_3N_4 photocatalysts co-doped with iron and phosphorus. Appl Surf Sci. 2014;311:164-171.
33. Liu G, et al. Unique electronic structure induced high photoreactivity of sulfur-doped graphitic C_3N_4. J Am Chem Soc. 2010;132:11642-11648.
34. Guo Q, et al. Engineering the electronic structure and optical properties of g-C_3N_4 by non-metal ion doping. J Mater Chem C. 2016;4: 6839–6847.
35. Liu Y, et al. State of the art of biogranulation technology for wastewater treatment. 2018;22:533–563.
36. Shen XZ, et al. Degradation of nitrobenzene using titania photocatalyst co-doped with nitrogen and cerium under visible light illumination. J Hazard Mater. 2009;162:1193-1198.
37. Muñoz-Batista MJ, et al. Effect of g-C_3N_4 loading on TiO_2-based photocatalysts: UV and visible degradation of toluene. Catal Sci Technol. 2014;4:2006-2015.
38. Fan G, et al. Coupling of Bi_2O_3 nanoparticles with g-C_3N_4 for enhanced photocatalytic degradation of methylene blue. Ceram Int. 2021;47:5758-5766.
39. Fu Y, et al. Ag/g-C_3N_4 catalyst with superior catalytic performance for the degradation of dyes: a borohydride-generated superoxide radical approach. Nanoscale. 2015;7:13723-13733.
40. Ismael M. A review on graphitic carbon nitride (g-C_3N_4) based nanocomposites: Synthesis, categories, and their application in photocatalysis. J Alloys Compd. 2020;846:156446.
41. Cheng F, et al. Low-temperature solid-state preparation of ternary CdS/g-C_3N_4 /CuS nanocomposites for enhanced visible-light photocatalytic H_2-production activity. Appl Surf Sci. 2007;391:432-439.
42. Zhu W, et al. Construction of WO_3-g-C_3N_4 composites as efficient photocatalysts for pharmaceutical degradation under visible light. Catal Sci Technol. 2017;7:2591-2600.
43. Ge L, et al. Enhanced visible light photocatalytic activity of novel polymeric g-C_3N_4 loaded with Ag nanoparticles. Appl Catal A: Gen. 2011;409–410:215-222.
44. He Y, et al. High-efficiency conversion of CO_2 to fuel over ZnO/g-C_3N_4 photocatalyst. Appl Catal B. 2015;168-169:1-8.

45. Zhou D, et al. Improved visible light photocatalytic activity on Z-scheme g-C_3N_4 decorated TiO_2 nanotube arrays by a simple impregnation method. Mater Res Bull. 2020;124:110757.
46. Xu M, et al. Facile fabrication of highly efficient g-C_3N_4/Ag_2O heterostructured photocatalysts with enhanced visible-light photocatalytic activity. ACS Appl Mater Interfaces. 2013;5:12533-12540.
47. Paul AM, et al. Cuprous oxide (Cu_2O)/graphitic carbon nitride (g-C_3N_4) nanocomposites for electrocatalytic hydrogen evolution reaction. Diam Relat Mater. 2020; 107:107899.
48. Ghane N, et al. Combustion synthesis of g- C_3N_4/Fe_2O_3 nanocomposite for superior photoelectrochemical catalytic performance. Appl Surf Sci. 2020;534:147563.
49. Cao SW, et al. Solar-to-fuels conversion over In_2O_3/g-C_3N_4 hybrid photocatalysts. Appl Catal B. 2014;147:940-946.
50. Li XH, et al. Metal-free activation of dioxygen by graphene/g-C_3N_4 nanocomposites: Functional dyads for selective oxidation of saturated hydrocarbons. J Am Chem Soc. 2011;133:8074-8077.
51. Wang X, et al. A metal-free polymeric photocatalyst for hydrogen production from water under visible light. Nature Materials. 2009; 8:76-80.
52. Iqbal W, et al. Controllable synthesis of graphitic carbon nitride nanomaterials for solar energy conversion and environmental remediation: The road travelled and the way forward. Catal Sci Technol. 8:4576-4599.
53. Sudhaik A, et al. Review on fabrication of graphitic carbon nitride based efficient nanocomposites for photodegradation of aqueous phase organic pollutants. Ind Eng Chem Res. 2018;67:28-51.
54. Lan ZA, et al. A facile synthesis of Br-modified g-C_3N_4 semiconductors for photoredox water splitting. Appl Catal B.2016; 192:116-125.
55. Zhang G, et al. Polycondensation of thiourea into carbon nitride semiconductors as visible light photocatalysts. J Mater Chem. 2012;22:8083-8091.
56. Chava RK, et al. Strategy for improving the visible photocatalytic H_2 evolution activity of 2D graphitic carbon nitride nanosheets through the modification with metal and metal oxide nanocomponents. Appl Catal B. 2019;248:538-551.
57. Xia X, et al. Preparation of magnetic graphitic carbon nitride nanocomposites. Mat Lett. 2010; 64: 2620-2623.
58. Shiraishi Y, et al. Effects of Surface Defects on Photocatalytic H_2O_2 Production by Mesoporous Graphitic Carbon Nitride under Visible Light Irradiation. ACS Catalysis. 2015;5:3058-3066.
59. Niu P, et al. Nitrogen vacancy-promoted photocatalytic activity of graphitic carbon nitride. J Phys Chem C. 2012;116:11013-11018.
60. Fang J, et al. “Dyed” graphitic carbon nitride with greatly extended visible-light-responsive range for hydrogen evolution. J Catal. 2016;339:93-101.
61. Reddy LN, et al. Graphitic carbon nitride–based nanocomposite materials for photocatalytic hydrogen generation. Nanostructured, Functional, and Flexible Materials for Energy Conversion and Storage Systems. 2020;9: 293-324.
62. Zhang J, et al. Synthesis of carbon nitride semiconductors in sulfur flux for water photoredox catalysis. Acs Catalysis. 2012;2:940-948.
63. Cui Y, et al. Synthesis of bulk and nanoporous carbon nitride polymers from ammonium thiocyanate for photocatalytic hydrogen evolution. J Mater Chem. 2011;21:13032-13039.

64. Yan SC, et al. Photodegradation performance of g-C_3N_4 fabricated by directly heating melamine. Langmuir. 2009;25:10397-10401
65. Ghosh U, et al. Photocatalytic CO_2 reduction over g-C_3N_4 based heterostructures: Recent progress and prospects. J Environ Chem Eng. 2021;9:104631.
66. Reddy IN, et al. Photoelectrochemical Studies on Metal-Doped Graphitic Carbon Nitride Nanostructures under Visible-Light Illumination. Catalysts. 2020;10:983.
67. Tseng TK, et al. A Review of Photocatalysts Prepared by Sol-Gel Method for VOCs Removal. Int J Mol Sci. 2010;11:2336-2361.
68. Xu B, et al. Graphitic carbon nitride based nanocomposites for the photocatalysis of organic contaminants under visible irradiation: Progress, limitations and future directions. Sci Total Environ. 2018;633:546-559.
69. Jiang L, et al. Phosphorus- and sulfur-codoped g-C_3N_4: facile preparation, mechanism insight, and application as efficient photocatalyst for tetracycline and methyl orange degradation under visible light irradiation. ACS Sustain Chem Eng. 2017;5:5831-5841.
70. Zhang Y, et al. Synthesis and luminescence mechanism of multicolor-emitting g-C_3N_4 nanopowders by low temperature thermal condensation of melamine. Scientific Reports. 2013;3:1-8.
71. Chen X, et al. Fe-g-C_3N_4-Catalyzed oxidation of benzene to phenol using hydrogen peroxide and visible light. J AM CHEM SOC. 2009;131:11658-11659.
72. Tonda S, et al. Fe-doped and -mediated graphitic carbon nitride nanosheets for enhanced photocatalytic performance under natural sunlight. J Mater Chem A. 2014;2: 6772–6780.
73. Gao J, et al. One-Pot Synthesis of copper-doped graphitic carbon nitride nanosheet by heating cu- melamine supramolecular network and its enhanced visible-light-driven photocatalysis. J Solid State Chem. 2015;228: 60-64.
74. Qin J, et al. Photocatalytic reduction of CO_2 by graphitic carbon nitride polymers derived from urea and barbituric acid. Appl Catal B. 2015;179:1-8.
75. Zhang G, et al. Dispersing molecular cobalt in graphitic carbon nitride frameworks for photocatalytic water oxidation. Small. 2015;11:1215-1221.
76. Le S, et al. Cu-doped mesoporous graphitic carbon nitride for enhanced visible-light driven photocatalysis. RSC Advances. 2016;6:38811-38819.
77. Lu C, et al. Boron doped g-C_3N_4 with enhanced photocatalytic UO22+ reduction performance. Appl Surf Sci. 2016;360:1016-1022.
78. Jiang J, et al. A comparison study of alkali metal - doped g- C_3N_4 for visible - light photocatalytic hydrogen evolution. Chinese J Catal. 2017;38:1981-1989.
79. Xiong T, et al. Bridging the g-C_3N_4 Interlayers for Enhanced Photocatalysis. ACS Catal. 2016; 6:2462-2472.
80. Das D, et al. Nickel doped graphitic carbon nitride nanosheets and its application for dye degradation by chemical catalysis. Mater Res Bull. 2018;101:291-304.
81. Fronczak M, et al. Extraordinary adsorption of methyl blue onto sodium-doped graphitic carbon nitride. J Phys Chem C. 2017;121:15756-15766.
82. Zhao J, et al. Novel band gap-tunable K–Na co-doped graphitic carbon nitride prepared by molten salt method. Appl Surf Sci. 2015;332:625-630.

83. Zhou Y, et al. Brand new P-doped g-C_3N_4: enhanced photocatalytic activity for H_2 evolution and Rhodamine B degradation under visible light. J Mater Chem A. 2015;3:3862-3867.
84. Lu C, et al. Photocatalytic reduction elimination of UO22+ pollutant under visible light with metal-free sulfur doped g-C_3N_4 photocatalyst. Appl Catal B. 2017;200:378-385.
85. Sagara N, et al. Photoelectrochemical CO_2 reduction by a p-type boron-doped g-C_3N_4 electrode under visible light. Appl Catal B. 2016;192:193-198.
86. Wang N, et al. A fluorescent probe using phosphorus-doped graphite carbon nitride nanosheets for the detection of silver ions and cell imaging. Can J Chem. 2020;98:408-414.
87. Zhang G, et al. Enhanced photocatalytic performance of boron and phosphorous co-doped graphitic carbon nitride nanosheets for removal of organic pollutants. Sep Purif Technol. 2019;226:128-137.
88. Niu P, et al. Graphene-like carbon nitride nanosheets for improved photocatalytic activities. Adv Funct Mater. 2012;4763-4770.
89. Thaweesak S, et al. Boron-doped graphitic carbon nitride nanosheets for enhanced visible light photocatalytic water splitting. Dalton Transactions. 2017; 46:10714-10720.
90. Qin Z, et al. Zinc-doped g- C_3N_4/$BiVO_4$ as a Z-scheme photocatalyst system for water splitting under visible light. Chinese J Catal. 2018;39:472-478.
91. Singh H, et al. Graphitic carbon nitride nanosheets (g-C_3N_4NS) as dual responsive template for fluorescent sensing as well as degradation of food colorants. Food Chemistry. 2020;128451.
92. Wang L, et al. Graphitic carbon nitride-based photocatalytic materials: preparation strategy and application. ACS Sustainable Chem Eng. 2020;8:16048-16085.
93. Ma S, et al. Hydrogen production by photocatalytic water splitting. J Jpn Pet Inst. 2013;56:280-287.
94. Zhang, et al. Photocatalysis: fundamentals, materials and applications. Springer. 2018.
95. Qi K, et al. A review on TiO_2 - based Z - scheme photocatalysts. Chinese J Catal. 2017; 38:1936-1955.
96. Cao S, et al. Facet effect of Pd cocatalyst on photocatalytic CO_2 reduction over g-C_3N_4. J Catal. 2017;349:208–217.
97. Sun Z, et al. g-C_3N_4 based composite photocatalysts for photocatalytic CO_2 reduction. Catalysis Today. 2018;300:160-172.
98. Samanta S, et al. Surface modified C, O co-doped polymeric g-C_3N_4 as an efficient photocatalyst for visible light assisted CO_2 reduction and H_2O_2 production. Appl Catal B. 2019;259:118054.
99. Guo L, et al. Z-scheme g- C_3N_4/$Bi_2O_2[BO_2(OH)]$ heterojunction for enhanced photocatalytic CO_2 reduction. J Colloid Interface Sci. 2020;568:139-147.
100. Xu D, et al. Ag_2CrO_4/g-C_3N_4/graphene oxide ternary nanocomposite Z-scheme photocatalyst with enhanced CO_2 reduction activity. Appl Catal B. 2018; 231:368–380.
101. Murugesan P, et al. Experimental studies on photocatalytic reduction of CO_2 using AgBr decorated g-C_3N_4 composite in TEA mediated system. J CO_2 Util. 2017; 22:250-261.
102. Huang D, et al. Graphitic carbon nitride-based heterojunction photoactive nanocomposites: applications and mechanism insight. ACS Appl Mater Interfaces. 2018;10:21035-21055.
103. Chai B, et al. Enhanced visible light photocatalytic degradation of Rhodamine B over phosphorus doped graphitic carbon nitride. Appl Surf Sci. 2017;391:376-383.

104. Vattikuti SVP, et al. Visible-light-driven photocatalytic activity of SnO_2-ZnO quantum dots anchored on g-C_3N_4 nanosheets for photocatalytic pollutant degradation and H_2 production. ACS Omega. 2018;3:7587-7602.

105. Konstas PS, et al. Synthesis, characterization of g-C_3N_4/$SrTiO_3$ heterojunctions and photocatalytic activity for organic pollutants degradation. Catalysts. 2018;8:554

106. Nagajyothi PC, et al. Enhanced photocatalytic activity of Ag/g-C_3N_4 composite. Sep Purif Technol. 2017;188:228-237.

107. Ma R, et al. Enhanced visible-light-induced photoactivity of type-ii CeO_2/g-C_3N_4 nanosheet toward organic pollutants degradation. ACS Sustain Chem Eng. 2019;7:9699-9708.

108. Hu S, et al. Band gap-tunable potassium doped graphitic carbon nitride with enhanced mineralization ability. Dalton Trans. 2015;44:1084-1092.

109. Liu J, et al. Uniform graphitic carbon nitride nanorod for efficient photocatalytic hydrogen evolution and sustained photoenzymatic catalysis. ACS Appl Mater Interfaces. 2014;6:8434-8440.